Available online at www.sciencedirect.com
ScienceDirect
Developmental Biology 314 (2008) 71–83
DEVELOPMENTAL BIOLOGY
www.elsevier.com/developmentalbiology

Loss of *Fgfr2* leads to partial XY sex reversal

Stefan Bagheri-Fam [a], Helena Sim [a], Pascal Bernard [a], Irumini Jayakody [b], Makoto M. Taketo [c], Gerd Scherer [d], Vincent R. Harley [a,*]

[a] *Human Molecular Genetics laboratory, Prince Henry's Institute of Medical Research, Monash Medical Centre, Melbourne 3168, Australia*
[b] *Department of Anatomy and Developmental Biology, Monash University, Melbourne 3800, Australia*
[c] *Department of Pharmacology, Graduate School of Medicine, Kyoto University, Yoshida-Konoé-cho, Kyoto 606-8501, Japan*
[d] *Institute of Human Genetics and Anthropology, University of Freiburg, D-79106 Freiburg, Germany*

Received for publication 5 October 2007; revised 5 November 2007; accepted 8 November 2007
Available online 19 November 2007

Abstract

In mammals, sex is determined in the bipotential embryonic gonad by a balanced network of gene actions which when altered causes disorders of sexual development (DSD, formerly known as intersex). In the XY gonad, presumptive Sertoli cells begin to differentiate when SRY up-regulates SOX9, which in turn activates FGF9 and PGDS to maintain its own expression. This study identifies a new and essential component of FGF signaling in sex determination. *Fgfr2* mutant XY mice on a mixed 129/C57BL6 genetic background had either normal testes, or developed ovotestes, with predominantly testicular tissue. However, backcrossing to C57BL6 mice resulted in a wide range of gonadal phenotypes, from hypoplastic testes to ovotestes with predominantly ovarian tissue, similar to *Fgf9* knockout mice. Since typical male-specific FGF9-binding to the coelomic epithelium was abolished in *Fgfr2* mutant XY gonads, these results suggest that FGFR2 acts as the receptor for FGF9. *Pgds* and SOX9 remained expressed within the testicular portions of *Fgfr2* mutant ovotestes, suggesting that the Prostaglandin pathway acts independently of FGFR2 to maintain SOX9 expression. We could further demonstrate that double-heterozygous *Fgfr2/Sox9* knockout mice developed ovotestes, demonstrating that both *Fgfr2* and *Sox9* can act as modifier intersex genes in the heterozygous state. In summary, we provide evidence that FGFR2 is important for male sex determination in mice, thereby rendering human *FGFR2* a candidate gene for unsolved DSD cases such as 10q26 deletions.

Keywords: Sex determination; XY sex reversal; SOX9; FGFR2; FGF9; PGDS; FGF signalling; Ovotestis; Disorders of sexual development; Testis

Introduction

In mammals, sex determination is chromosomally controlled, under the regulation of the sex-determining region of the Y chromosome gene (*SRY*), which encodes a sequence-specific DNA binding protein (Harley et al., 1992; Sinclair et al., 1990). The embryonic gonad normally develops into either a testis or an ovary, but in DSD cases (disorders of sexual development, formerly known as intersex; Hughes et al., 2006), an ovotestis can occur that contains both testicular and ovarian tissue (Brennan and Capel, 2004; Swain and Lovell-Badge, 1999). In humans, mutations in *SRY*, *SOX9*, *SF1*, *WT1* or *DHH* as well as duplications of *DAX1* or of *WNT4* can upset the balanced network of gene expression, causing XY gonadal dysgenesis or XY sex reversal (Fleming and Vilain, 2005). The majority of such DSD conditions, however, remain unexplained genetically.

Testis determination is best understood in the mouse. In the XY gonad, *Sry* is expressed in bipotential supporting cells (primordial Sertoli/follicle cells) at embryonic day 10.5 (E10.5) and by E11.5 SRY triggers Sertoli cell fate by activating the transcription of *Sox9* (Brennan and Capel, 2004; Swain and Lovell-Badge, 1999), an *Sry*-related, autosomal transcription factor gene. Once Sertoli cells have differentiated, other

Abbreviations: AMH, anti-Müllerian hormone; B6, C57BL6; *Bmp2*, bone morphogenetic protein 2; Ck19, cytokeratin 19; *Cyp26b1*, cytochrome P450 26b1; *Dmc1*, disrupted meiotic cDNA 1; DSD, disorders of sexual development; En, embryonic day n; FGF, fibroblast growth factor; FGFR, fibroblast growth factor receptor; *Fst*, follistatin; PGD2, prostaglandin D2; *Pgds*, prostaglandin D synthase; SCP3, synaptonemal complex protein 3; SOX9, SRY type high mobility group box 9; SRY, sex-determining region of the Y chromosome; *Stra8*, stimulated by retinoic acid gene 8; *Wnt4*, wingless-related MMTV integration site 4.

* Corresponding author. Fax: +61 3 95946125.
E-mail address: vincent.harley@princehenrys.org (V.R. Harley).

0012-1606/$ - see front matter © 2007 Elsevier Inc. All rights reserved.
doi:10.1016/j.ydbio.2007.11.010

bipotential cell types of the gonad (Leydig/theca, male/female germ cells) become committed to the male pathway (McLaren and Southee, 1997).

Mutations in human *SOX9* lead to campomelic dysplasia, a skeletal malformation syndrome with associated XY sex reversal in two thirds of all XY cases (Foster et al., 1994; Wagner et al., 1994). Mice lacking *Sox9*, like those lacking Fibroblast growth factor 9 (*Fgf9*), undergo XY male-to-female sex reversal as a consequence of the perturbations to early male-specific events of gonad development (Barrionuevo et al., 2006; Chaboissier et al., 2004; Colvin et al., 2001; Kim et al., 2006; Schmahl et al., 2004). *Sox9* is essential for expression of FGF9 which acts to maintain *Sox9* expression by an unknown mechanism (Kim et al., 2006). FGF9 in turn inhibits the female pathway by down-regulating the expression of *Wnt4*.

The receptor that mediates FGF9 signals in sex determination is not known. FGF9 can bind to and activate all four FGF receptors (FGFR1–4) *in vitro* (Ornitz et al., 1996) and all four receptors are expressed in the somatic cells of XY and XX gonads at E11.5 (Schmahl et al., 2004). Chimeric *Fgfr1* knockout mice with 90% inactivation show normal testis development, and *Fgfr3* and *Fgfr4* knockout mice are fertile (Colvin et al., 1996; Deng et al., 1996, 1997; Weinstein et al., 1998), indicating that these receptors are either not required for sex determination, or they act redundantly. Rather unusually, FGFR2 protein is localized male-specifically in the nucleus of differentiating E11.5 Sertoli cells, co-incident with elevated SOX9 protein expression (Schmahl et al., 2004). Therefore, *Fgfr2* is a good candidate sex determining gene.

Hitherto the obstacle to studying FGFR2 sex-determining function has been that homozygous *Fgfr2* knockout mice die before sex determination occurs due to extraembryonic defects (Xu et al., 1998). We circumvented this by conditionally inactivating *Fgfr2* only in the embryo proper. We show that FGFR2 is important for male sex determination since *Fgfr2* mutant XY mice, with gonadal phenotypes similar to *Fgf9* knockout mice, and *Fgfr2/Sox9* double heterozygous XY knockout mice show gonadal male-to-female sex reversal. Since we show that FGF9 does not bind to the coelomic epithelium of *Fgfr2* mutant XY gonads, our data support FGFR2 being the receptor for FGF9.

Results

Conditional homozygous inactivation of Fgfr2 in the gonad

Complete *Fgfr2* knockout mice die at around E10.5 prior to sex determination, due to a malfunction in chorioallantoic fusion or placental development (Xu et al., 1998). To circumvent early embryonic lethality of complete *Fgfr2* knockout mice, we used a conditional gene knockout approach using the *Ck19:Cre* mouse line, which expresses Cre-recombinase between E4.5 and E5.5 only in the embryo proper (epiblast) (Means et al., 2005). We have shown previously by using the *Ck19:Cre* line to inactivate *Sox9*, that gene inactivation was highly efficient within the E11.5 XY male genital ridge and that most *Sox9* mutant XY embryos displayed complete male-to-female sex reversal (Barrionuevo et al., 2006). $Fgfr2^{flox/flox}$ mice bred on a mixed 129/C57BL6 genetic background (Yu et al., 2003) were crossed with the *Ck19:Cre/+* (C57BL6) transgenic mouse line (Means et al., 2005) to generate $Ck19:Cre/+;Fgfr2^{flox/+}$ offspring. These mice did not show an obvious phenotype and were backcrossed to $Fgfr2^{flox/flox}$ mice to obtain $Ck19:Cre/+;Fgfr2^{flox/flox}$ ('*Fgfr2* mutant') embryos.

Fgfr2 mutant embryos were recovered at the expected Mendelian ratio, but died immediately after birth. *Fgfr2* mutants showed variable limb defects ranging from malformed and shortened limbs to absence of limbs (Fig. 1A), reflecting moderate to complete inactivation of the *Fgfr2* gene. The latter phenotype resembles that of complete *Fgfr2* knockout embryos, which also lack limbs (Xu et al., 1998). Immunohistochemistry for FGFR2 at E12.5 revealed a drastic reduction of FGFR2-positive Sertoli cells in *Fgfr2* mutant XY gonads (70–100% inactivation; see Fig. 1B for details), indicating that *Fgfr2* inactivation was efficient (Fig. 1B).

Fgfr2 mutant XY gonads on a mixed 129/B6 background show defects in testis cord formation

At E13.5, the XY male gonad is characterized by the formation of the presumptive seminiferous tubules, known as testis cords (Figs. 2A and B). To analyze if *Fgfr2* mutant XY mice show defects in testis cord formation, we performed gross morphological and histological analyses of XY *Fgfr2* mutant, and XY and XX wild type gonads between E13.5 and E15.5. 25% of *Fgfr2* mutant XY mice (10 gonads; 4 at E13.5, 4 at E14.5 and 2 at E15.5) had normal testes (data not shown), while 75% (28 gonads; 14 at E13.5, 10 at E14.5 and 4 at E15.5) showed defects in testis cord formation of varying severity (Figs. 2A and B and data not shown). At E13.5 and E14.5, in *Fgfr2* XY mutants, testis cords were formed properly at the center of the gonad (Fig. 2A and data not shown), whereas the anterior pole (arrow in Fig. 2A), and less frequently the posterior pole, contained either highly disorganized cords or had an unstructured appearance similar to a female gonad (Figs. 2A and B, and Fig. 4B(i)) (see Fig. 2 for details). By E15.5, the gonads appeared as ovotestes with the ovarian portion predominantly located at the anterior pole of the gonad (arrow in Fig. 2A). The postnatal development of *Fgfr2* mutant gonads could not be studied, since the *Fgfr2* mutant mice die at birth. It should be noted that of six embryos analyzed we did not observe a significant correlation between the efficiency of FGFR2 inactivation (number of remaining FGFR2-positive cells) and the severity of the phenotype (normal testis or ovotestis) (see Fig. 1B for details), suggesting that the gonadal phenotype might vary more strongly with other factors, such as the genetic background of this mixed 129/C57BL6 mouse strain. In summary, XY *Fgfr2* mutant male gonads failed to form testis cords at the gonad poles, leading to ovotestis formation.

Fgfr2 mutants show partial XY sex reversal

To investigate the course of gonadal sex reversal induced by FGFR2 loss, we undertook a molecular analysis of *Fgfr2* XY

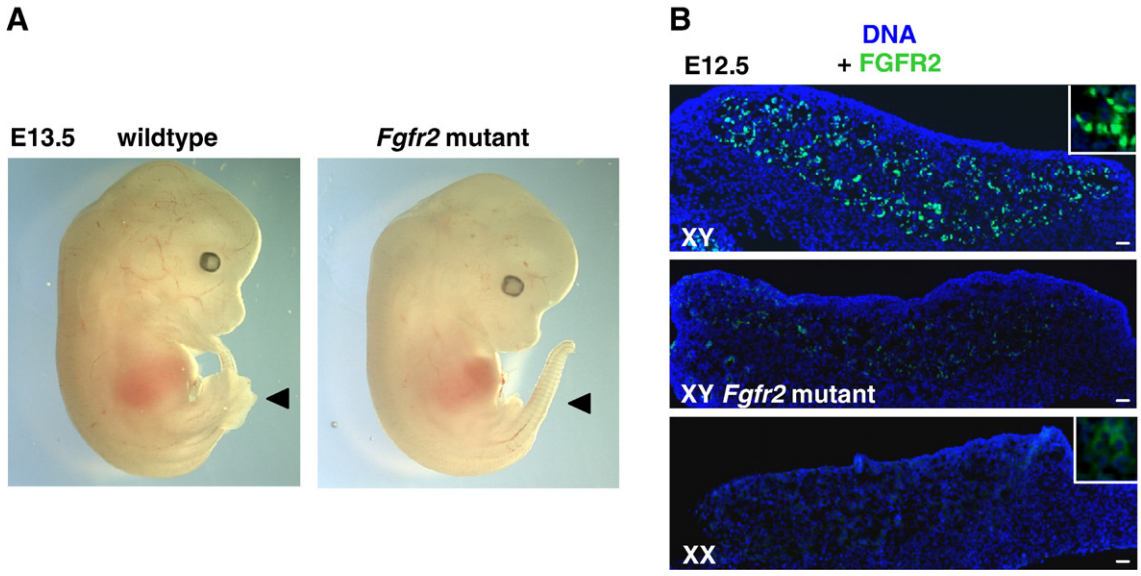

Fig. 1. Conditional inactivation of *Fgfr2* using *Ck19:Cre*. (A) Limb bud defects in *Fgfr2* mutant embryos at E13.5. Arrowheads point to the hindlimbs, which are absent in severely affected *Fgfr2* mutant embryos. (B) Immunohistochemistry of frozen sections of *Fgfr2* mutant XY and control gonads at E12.5 with an antibody against FGFR2. The inserts in the *top* and *bottom panels* show magnifications of cells stained for DAPI (blue, nuclear) and FGFR2 (green, nuclear in the wild type XY gonad and at the membrane in the wild type XX gonad). Efficiency of *Fgfr2* inactivation was determined by counting the number of FGFR2-positive Sertoli cells per section over four sections (more than 100 cells) in XY wild type and *Fgfr2* mutant XY gonads. A total of six gonads from six different embryos have been analyzed, revealing a drastic reduction of FGFR2-positive Sertoli cells (between 70% and 100% per gonad) in *Fgfr2* mutant XY embryos. It should be noted that we did not observe a significant correlation between the efficiency of FGFR2 inactivation (number of remaining FGFR2-positive Sertoli cells) and the severity of the phenotype (normal testis or ovotestis). Of the six E12.5 *Fgfr2* mutant XY gonads analyzed, two were normal testes (approximately 70% and 100% inactivation), while four were ovotestes (approximately 70% (2 gonads), 80% and 100% inactivation). Scale bars are 50 μm.

mutants. At E11.5, both wild type XY and *Fgfr2* mutant XY embryos showed strong SRY and SOX9 protein expression, indicating proper initiation of male sex determination (Fig. 3A). However, by E12.5, while in wild type XY embryos, SOX9 and AMH, a direct SOX9 target and specific marker of Sertoli cells, were strongly co-expressed throughout the gonad; in *Fgfr2* mutant XY gonads, the number of SOX9- and AMH-positive cells was reduced near the poles of the gonad, particularly near the anterior pole (Fig. 3B). Moreover, in contrast to SOX9-expression levels (Fig. 3B, middle panel), AMH-expression levels were drastically reduced at the poles (Fig. 3B, bottom panel). By E14.5, SOX9 (Fig. 3C, upper panel) and AMH (Fig. 3C, lower panel) were absent at the poles, indicating a failure of Sertoli cell differentiation at this location.

To investigate whether the poles of the *Fgfr2* mutant male gonads underwent a fate change and developed along the female pathway, we analyzed the expression of the ovarian somatic cell markers *Wnt4* and *Fst* (Follistatin), by whole mount *in situ* hybridization. *Wnt4* is down-regulated by FGF9 during male gonadal development (Kim and Capel, 2006; Kim et al., 2006) and is one of the earliest known female markers (Vainio et al., 1999), while *Fst* is a downstream component of Wnt4 signaling (Yao et al., 2004). Wild type XY male gonads showed no *Wnt4* and *Fst* expression, whereas XX female gonads displayed strong *Wnt4* and *Fst* expression throughout the entire gonad at E12.5 and E14.5, respectively (Fig. 4A). *Fgfr2* mutant XY gonads showed *Wnt4* and *Fst* expression specifically at their poles, indicating that the somatic cells at the poles develop along the female pathway (arrow in Fig. 4A).

Mouse primordial germ cells proliferate until E13.5, then enter into meiotic prophase in the female gonad or become mitotically arrested in the male gonad (Hilscher et al., 1974). To study the fate of germ cells in the *Fgfr2* mutant ovotestis, we first performed histological analyses of *Fgfr2* mutant XY gonads at E14.5 (Fig. 4B(i)). During meiotic prophase, the chromosomes coil and become shorter and thicker and visible under the light microscope. We found that, in *Fgfr2* mutant XY gonads, germ cells at the anterior pole, and less frequently at the posterior pole, appeared to have entered meiotic prophase (arrow in Fig. 4B(i)). This was confirmed by the expression specifically at the gonads poles of *Stra8* (encodes a pre-meiotic marker) (Menke et al., 2003), and of the meiotic prophase markers SCP3 (a component of the synaptonemal complex) and *Dmc1* (encodes a meiosis-specific recombinase) (Bullejos and Koopman, 2004; Chuma and Nakatsuji, 2001; Di Carlo et al., 2000; Menke et al., 2003) at the gonad poles (Fig. 4B(ii)). Retinoic acid, produced by mesonephroi of both sexes, causes germ cells in the ovary to enter meiosis and initiate oogenesis. In the fetal testis, Sertoli cells secrete the retinoid-degrading enzyme CYP26B1 thereby preventing meiosis, ultimately leading to spermatogenesis (Bowles et al., 2006; Koubova et al., 2006). In *Fgfr2* mutant XY gonads *Cyp26b1* expression was absent from the gonad poles (Fig. 4B(ii), bottom panel), which might explain why meiosis is restricted to the polar regions. Taken together, the presence of the somatic female markers *Wnt4* and *Fst*, and of the pre-meiotic/meiotic markers *Stra8*, *Dmc1* and SCP3, strongly suggests that the poles of the *Fgfr2* mutant XY gonads are sex-reversed.

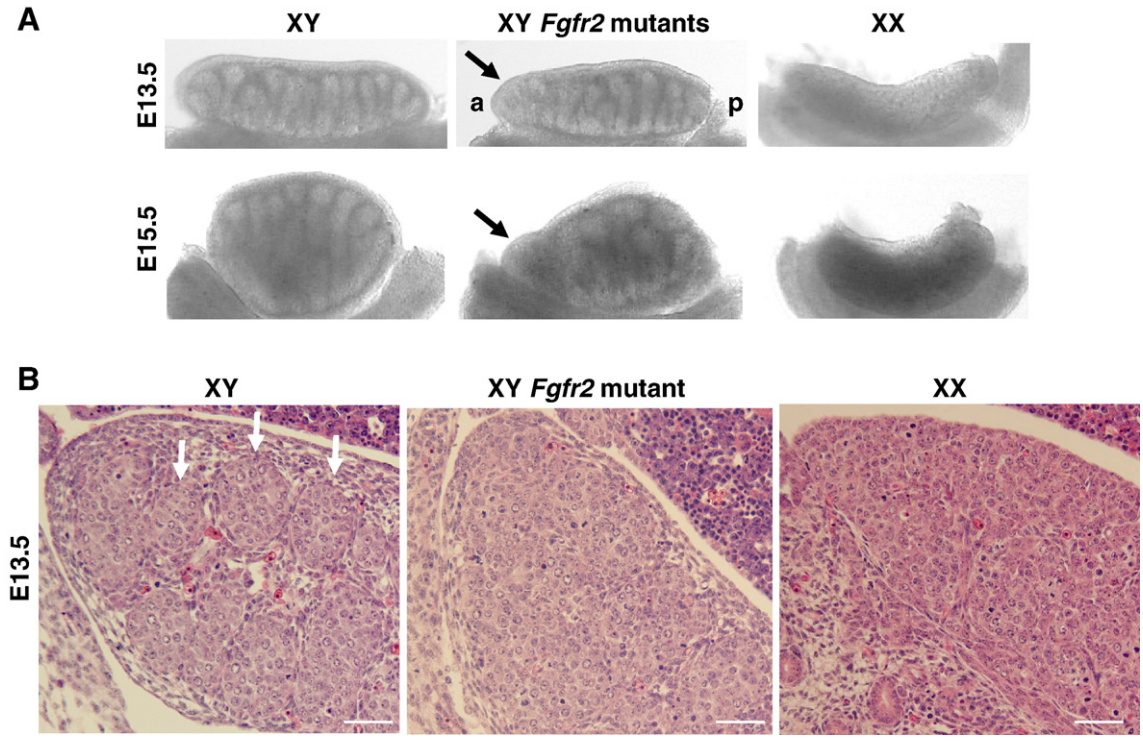

Fig. 2. *Fgfr2* mutant XY gonads show defects in testis cord formation. (A) Light microscopy images of *Fgfr2* mutant XY and control gonads at E13.5 and E15.5. In wild type XY gonads, testis cords (bright regions) are visible through a light microscope, which are separated by peritubular tissue (dark regions). At the anterior pole of *Fgfr2* mutant XY gonads (arrows), testis cords were poorly distinguished from the peritubular tissue or appeared to be absent. (B) Hematoxylin and eosin (HE) staining of sections of paraffin-embedded mutant and control embryos at E13.5 (Enlargements of the anterior regions of the gonads are shown). In wild type XY gonads, testis cords (arrows point to examples of well formed testis cords) are separated by interstitial cells that define the peritubular space. Sertoli cells are present at the periphery of the tubule and peritubular myoid (PTM) cells form a concentric layer of cells that surrounds the testis cord. Between PTM and Sertoli cells, a basal lamina is formed which is visible as a thin line. The anterior pole of *Fgfr2* mutant XY gonads contained either highly disorganized cords (as judged by the reduced number of PTM cells and the lack of the basal lamina separating cords from the peritubular space), or had an unstructured appearance similar to a female gonad. a, anterior; p, posterior. Scale bars are 50 μm.

The mouse strain C57BL6 exacerbates XY sex reversal of Fgfr2 mutant XY gonads

The sex-reversal phenotype of *Fgfr2* mutant XY gonads was milder than that of *Fgf9* knockout XY mice which were also bred on a mixed 129/C57BL6 background (Colvin et al., 2001). This may be attributable to differing genetic contribution of the C57BL6 (B6) mouse strain, which is exquisitely sensitive to XY sex reversal, as shown in *Fgf9* and *Dax1* knockout mice (Bouma et al., 2005; Colvin et al., 2001; Meeks et al., 2003; Schmahl et al., 2004). To test whether the B6 mouse strain can exacerbate the XY sex-reversal phenotype of *Fgfr2* mutant gonads, we backcrossed *Ck19:Cre/+;Fgfr2*$^{flox/+}$ and *Fgfr2*$^{flox/flox}$ mice to B6. Resultant *Ck19:Cre/+;Fgfr2*$^{flox/+}$ (129/B6*) and *Fgfr2*$^{flox/+}$ (129/B6*) mice were crossed with each other to generate *Fgfr2* mutant (129/B6*) XY embryos. Gross morphological analyses at E14.5 revealed a range of gonadal phenotypes, from ovotestes with predominantly testicular tissue (8 gonads, data not shown), to ovotestes with predominantly ovarian tissue (5 gonads) (Fig. 5A), to gonads the size and shape of ovaries (3 gonads) (Fig. 5A). Gonads of the latter phenotype lacked the male-specific blood vessel altogether, while in ovotesticular gonads the blood vessel was restricted to a region above the testis cords (Fig. 5A). The anterior region of the gonads was always more severely affected than the posterior region. With increasing expressivity of the ovarian phenotype among *Fgfr2* mutant XY gonads, the male markers SOX9 and AMH were gradually lost from pole to center, particularly from the anterior pole (Figs. 5B and C, upper panel). In more dramatic phenotypes, only few testis cords remained (as evidenced by AMH-expression), restricted to a small region just posterior to the center of the gonad (Fig. 5B(ii), middle panel, and C, upper panel). Conversely, the female somatic cell marker *Bmp2* was specifically absent only from this restricted region (Fig. 5C, lower panel), confirming that these gonads were predominantly ovaries. In one gonad examined, we observed almost complete loss of SOX9 and AMH expressing cells (Fig. 5B(ii), bottom panel). These data demonstrate that the mouse strain C57BL6 exacerbates the phenotype of *Fgfr2* mutant XY gonads, leading to almost complete sex reversal in some cases.

Pgds expression persists in testis cords of Fgfr2 mutant and Fgfr2 mutant (129/B6) XY gonads*

Our data show that SOX9 can still be widely expressed in gonads lacking FGFR2 (Fig. 3C, upper panel and Fig. 5B(ii),

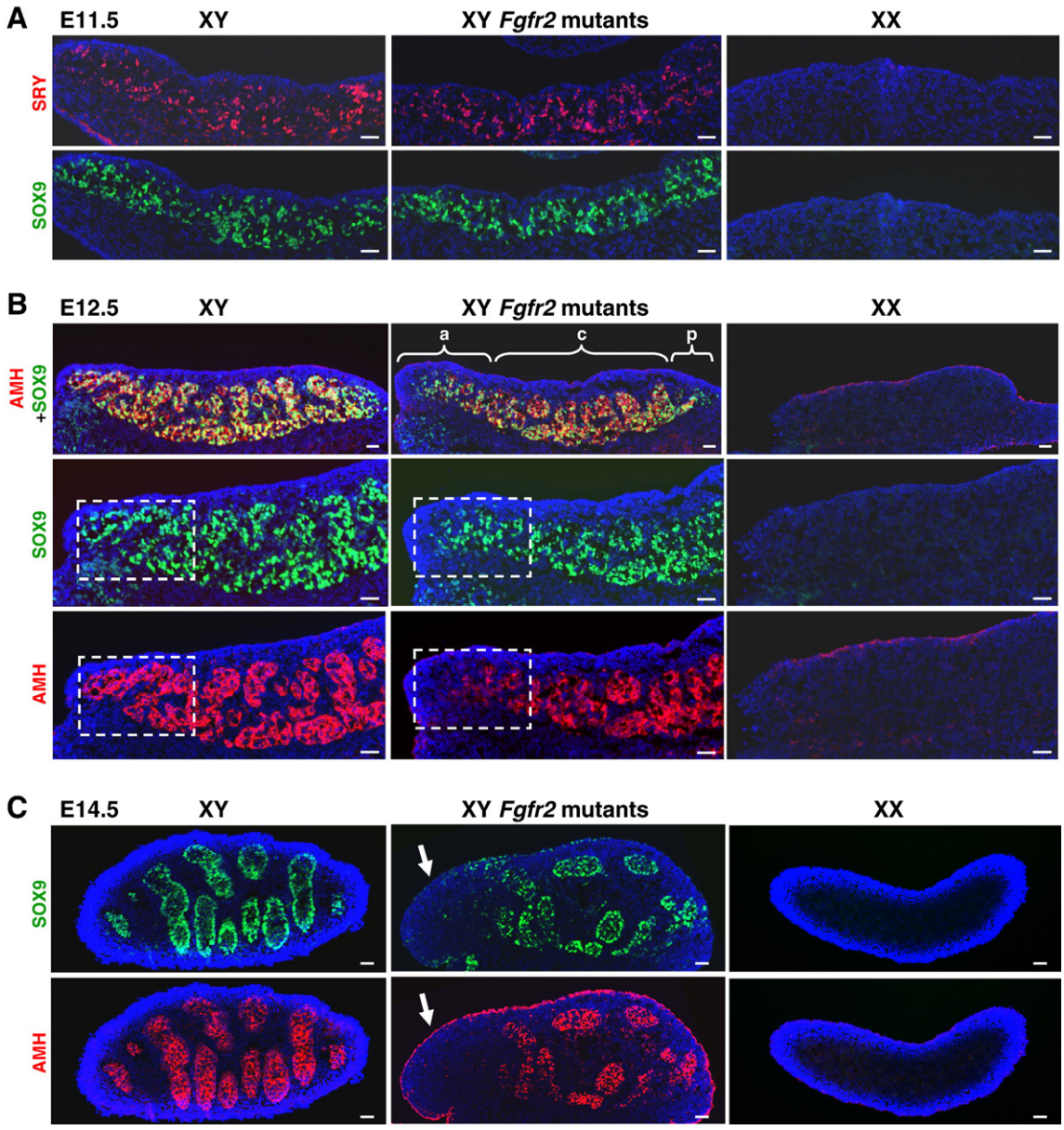

Fig. 3. The Sertoli cell markers SOX9 and AMH are reduced or absent from the poles of *Fgfr2* mutant XY gonads. (A) Fluorescence microscopy of frozen sections of *Fgfr2* XY mutant and control gonads at E11.5 immunostained for Sertoli cell markers, SRY (red, nuclear) (upper panel) and SOX9 (green, nuclear) (lower panel). SRY and SOX9 appear to be expressed normally in E11.5 *Fgfr2* XY mutants. (B) Top panel: Fluorescence microscopy of frozen sections of E12.5 *Fgfr2* mutant XY and control gonads double immunostained for SOX9 (green, nuclear) and AMH (red, cytoplasmic). The middle and bottom panels represent magnifications of the same gonad sections shown in the top panel in which the signals for SOX9 (middle panel) and AMH (bottom panel) have been separated. *Fgfr2* mutant XY gonads show a reduction of SOX9- and AMH-expressing cells near the poles of the gonad, particularly near the anterior pole. Over 100 SOX9-postive cells were counted in a defined field in the anterior region (framed in middle and bottom panels). There were approximately 50% fewer SOX9-positive cells in *Fgfr2* mutant XY gonads compared to XY control gonads ($n=5$). (C) Upper panel: Fluorescence microscopy of frozen sections of *Fgfr2* mutant XY and control gonads at E14.5 immunostained for SOX9 (green, nuclear). Lower panel: Fluorescence microscopy of frozen sections of *Fgfr2* mutant XY and control gonads at E14.5 immunostained for AMH (red, cytoplasmic). At E14.5, SOX9 and AMH are absent at the poles (arrow) of *Fgfr2* mutant XY gonads. a, anterior; c, center; p, posterior. All scale bars are 50 μm.

top panel), which implies that other mechanisms might maintain SOX9 expression. Evidence is emerging that SOX9 also participates in a SOX9–PGDS (Prostaglandin D Synthase)–PGD2 (Prostaglandin D2) positive loop. SOX9 directly regulates *Pgds* transcription *in vivo* (Wilhelm et al., 2007). Conversely, PGD2 promotes accumulation of SOX9 in the nucleus via an importin beta pathway as demonstrated by Malki et al. (2005); in cultured XX gonads, PGD2 can induce *Sox9* transcription (Wilhelm et al., 2005). Together, these data support a positive feedback loop between SOX9 and PGD2. To investigate whether the PGDS/PGD2-pathway might still be active within the testicular regions of *Fgfr2* mutant and *Fgfr2* mutant (129/B6*) XY gonads, we analyzed the expression of *Pgds* by whole mount *in situ* hybridization. At E13.5/E14.5, the XY gonad expresses *Pgds* in Sertoli cells of the testis cords, while the XX gonad does not express *Pgds*

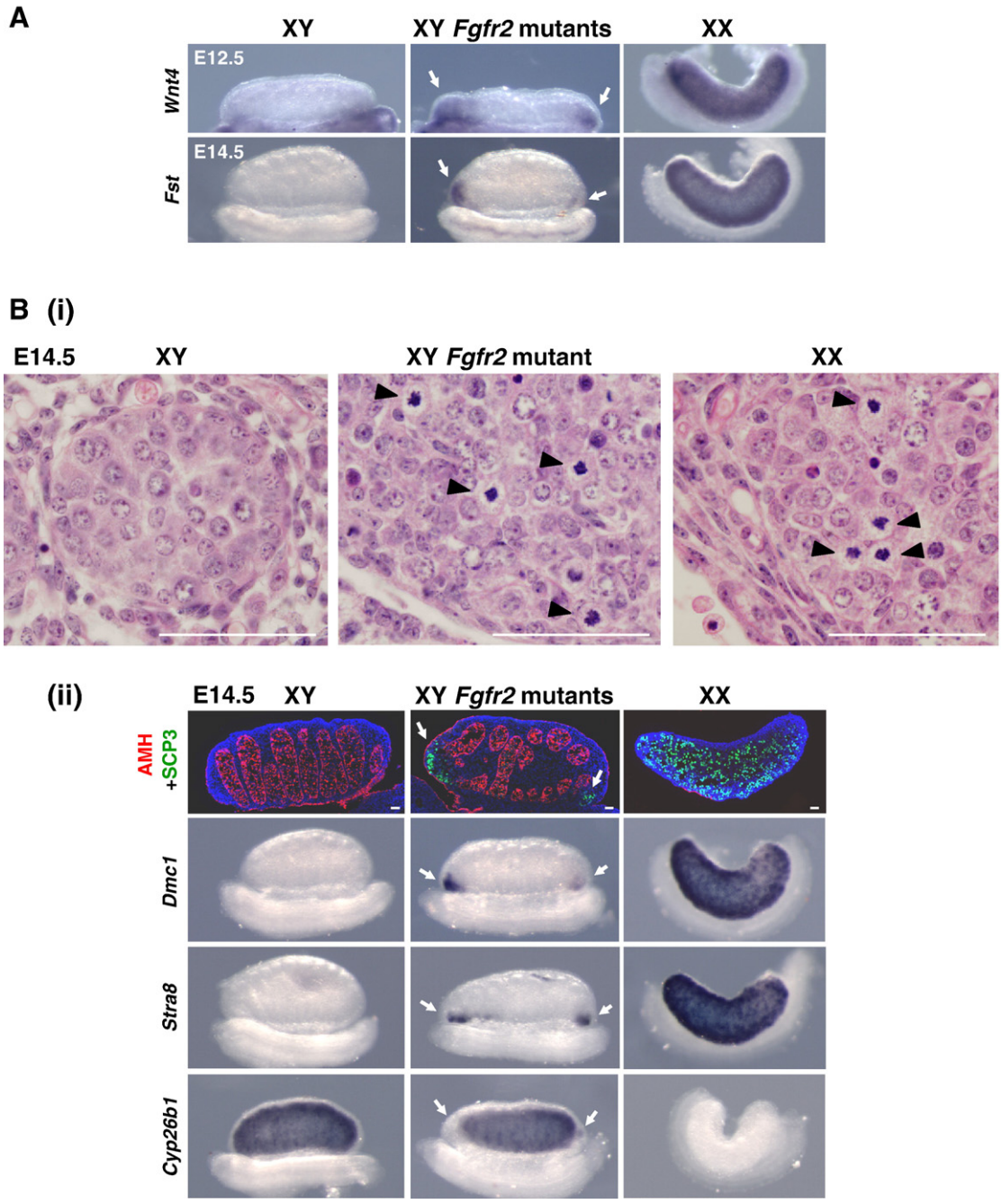

Fig. 4. The poles of *Fgfr2* mutant XY gonads develop along the female pathway. (A) Upper panel: Whole mount *in situ* hybridization for *Wnt4* of E12.5 *Fgfr2* mutant XY and control gonads. Lower panel: Whole mount *in situ* hybridization for the female somatic cell marker *Fst* of E14.5 *Fgfr2* mutant XY and control gonads. Arrows point to the *Wnt4*- and *Fst*-positive poles of the *Fgfr2* mutant XY gonads. (B) (i) Hematoxylin and eosin staining of sections of paraffin-embedded mutant and control embryos at E14.5 (Enlargements of the anterior regions of the gonads are shown). At the anterior pole of *Fgfr2* mutant XY gonads, testis cords are absent, and germ cells have entered prophase of meiosis (arrowheads). (ii) Top panel: Fluorescence microscopy of frozen sections of *Fgfr2* mutant XY and control gonads at E14.5 double immunostained for AMH (red, cytoplasmic) and SCP3 (green, nuclear), a marker of female meiotic germ cells. Second panel: Whole mount *in situ* hybridization for the meiotic marker *DmcI* of E14.5 *Fgfr2* mutant XY and control gonads. Third panel: Whole mount *in situ* hybridization for the pre-meiotic marker *Stra8* of E14.5 *Fgfr2* mutant XY and control gonads. Bottom panel: Whole mount *in situ* hybridization for *Cyp26b1* of E14.5 *Fgfr2* mutant XY and control gonads. Arrows denote the SCP3-, *DmcI*- and *Stra8*-positive and *Cyp26b1*-negative poles of *Fgfr2* mutant XY gonads. The presence of somatic female markers and of meiosis markers indicates that the poles of *Fgfr2* mutant XY gonads are sex reversed. All scale bars are 50 μm.

(Fig. 6). In *Fgfr2* mutant and in *Fgfr2* mutant (129/B6*) XY gonads, *Pgds* was still expressed within the testis cords, similar to SOX9 (Fig. 3C, upper panel and Fig. 5B(ii)). These data indicate that the SOX9–PGDS–PGD2 pathway acts independently of FGFR2.

FGF9 does not bind to the coelomic epithelium of Fgfr2 mutant XY gonads

It has been recently demonstrated that FGF9 binds to the coelomic surface of the E11.5 XY gonad (Schmahl et al.,

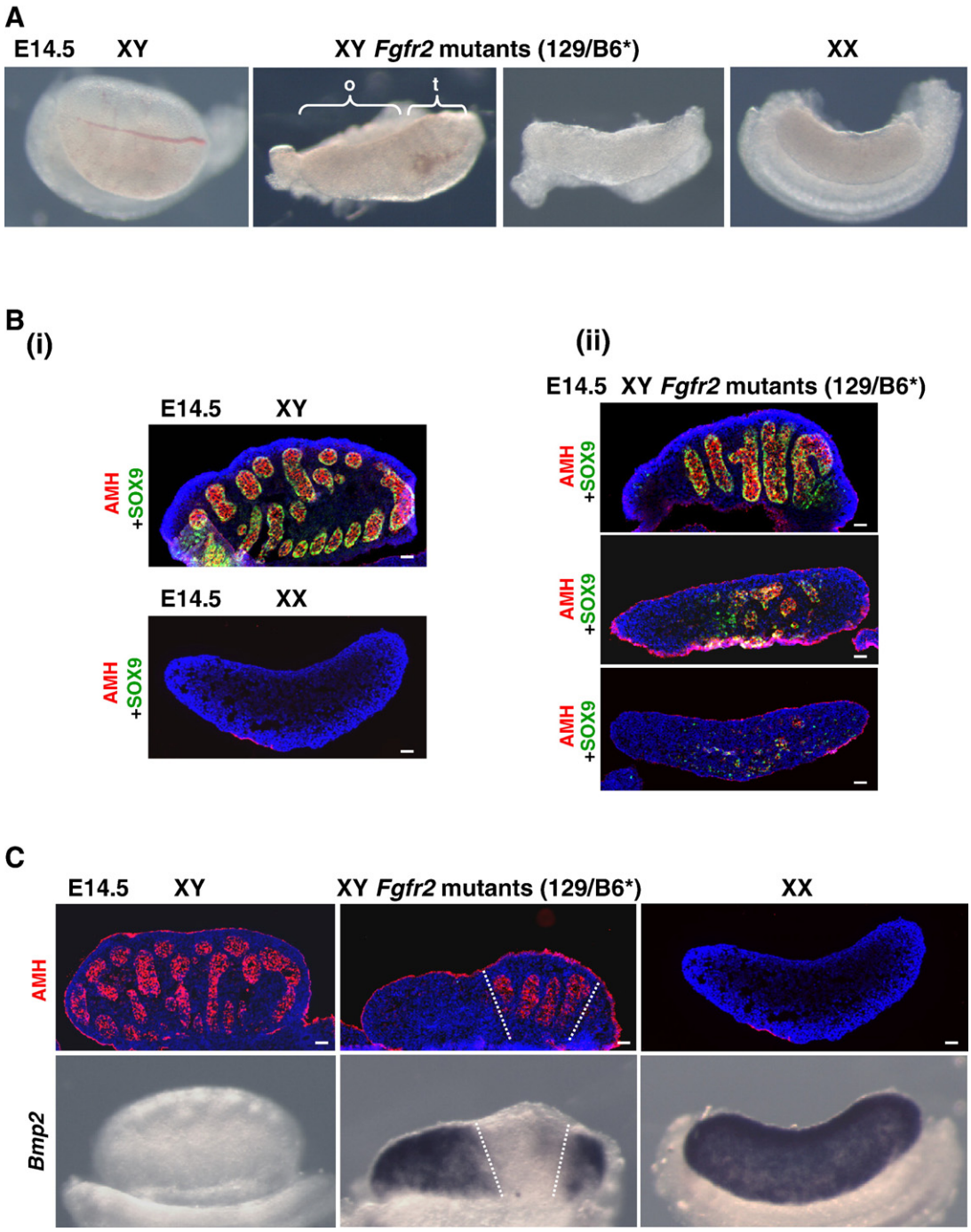

Fig. 5. C57BL6 exacerbates XY sex reversal of *Fgfr2* mutant XY gonads. (A) Light microscopy images of *Fgfr2* mutant (129/B6*) XY and control gonads at E14.5. *Fgfr2* mutant (129/B6*) XY gonads appear as ovotestes, or have a size and shape very similar to a female gonad. The male-specific coelomic blood vessel is restricted to regions with testis cords. (B) (i) Fluorescence microscopy of frozen sections of XY and XX control gonads at E14.5 double immunostained for SOX9 (green, nuclear and AMH (red, cytoplasmic). (ii) Top, middle and bottom panels: Fluorescence microscopy of frozen sections of *Fgfr2* mutant XY gonads at E14.5 (with increasing severity from top to bottom) double immunostained for SOX9 (green, nuclear) and AMH (red, cytoplasmic). (C) Upper panel: Fluorescence microscopy of frozen sections of *Fgfr2* mutant XY and control gonads at E14.5 immunostained for AMH (red, cytoplasmic). Lower panel: Whole mount *in situ* hybridization for *Bmp2* of E14.5 *Fgfr2* mutant XY and control gonads. Dotted lines denote the borders between ovarian and testicular tissue. o, ovarian portion of the *Fgfr2* mutant ovotestis; t, testicular portion of the *Fgfr2* mutant ovotestis. All scale bars are 50 μm.

2004). Since FGFR2 is expressed at the coelomic epithelium at this time, it has been speculated that FGF9 signals through FGFR2. In order to test whether FGF9 binding is abolished in *Fgfr2* mutant XY gonads, we performed *in situ* binding assays with human FGF9 as previously described (Schmahl et al., 2004). While FGF9 accumulated at the coelomic epithelium of E11.5 XY gonads, both XX and *Fgfr2* mutant XY gonads (3 pairs of gonads per genotype) did not

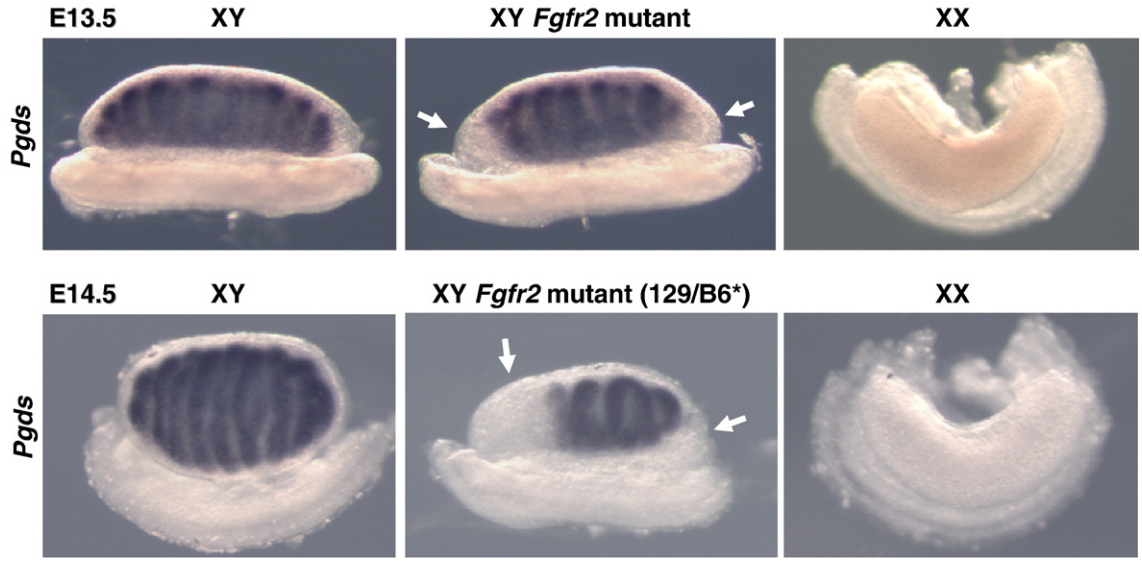

Fig. 6. Analysis of *Pgds* expression in *Fgfr2* mutant XY gonads. Upper panel: Whole mount *in situ* hybridization for *Pgds* of E13.5 *Fgfr2* mutant XY and control gonads. Lower panel: Whole mount *in situ* hybridization for *Pgds* of E14.5 *Fgfr2* mutant (129/B6*) XY and control gonads. Arrows point to the *Pgds*-negative regions of *Fgfr2* mutant and *Fgfr2* mutant (129/B6*) XY gonads. In *Fgfr2* mutant XY gonads, except for the poles, *Pgds* is still strongly expressed throughout the gonad, while in *Fgfr2* mutant (129/B6*) XY gonads, *Pgds* is lost from the anterior region of the gonad.

significantly bind human FGF9 (Fig. 7). However, it should be noted that due to the chimeric character of the *Ck19:Cre* mouse line, we occasionally observed FGF9 binding also in *Fgfr2* mutant XY gonads.

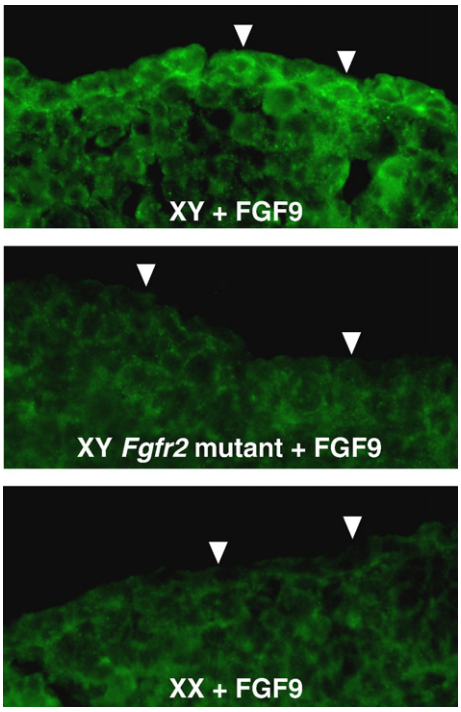

Fig. 7. FGF9 does not bind to the coelomic epithelium of *Fgfr2* mutant XY gonads. E11.5 gonad sections were incubated with human FGF9, which was detected with an antibody specific to the human FGF9 protein (green). Human FGF9 bound to the coelomic epithelium in E11.5 XY gonad sections, but not in E11.5 XX and XY *Fgfr2* mutant gonad sections. Arrowheads denote the surface of the coelomic epithelium.

FGFR2 nuclear localization is dependent on SOX9

Following SRY mediated up-regulation of SOX9 at E11.5, FGFR2 accumulates in the Sertoli cell nuclei of XY gonads (Schmahl et al., 2004). The importance of FGFR2 nuclear localization for Sertoli cell differentiation and testis development has been recently demonstrated by Kim et al. (2007). It has been previously shown that E11.5 *Sox9* knockout gonads do not express *Fgf9* (Kim et al., 2006), and that, in E12.5 *Fgf9* knockout gonads lacking SOX9, FGFR2 is not nuclear (Schmahl et al., 2004; Kim et al., 2006). However, FGFR2 nuclear localization in *Sox9* knockout gonads has not been studied. To test directly whether SOX9 affects the nuclear localization of FGFR2, we performed immunohistochemistry for FGFR2 in *Ck19:Cre/+*; $Sox9^{flox/flox}$ ('*Sox9* mutant') XY gonads at E11.5, the time when FGFR2 is normally translocated into the nucleus. Strong nuclear staining in pre-Sertoli cells of SRY, SOX9 and FGFR2 was observed in E11.5 wild type XY gonads, while in wild type XX gonads, only FGFR2 was detectable (Fig. 8), localized at the plasma membrane and in the cytoplasm. In *Sox9* mutant XY gonads, though SRY was expressed (Fig. 8, upper panel), FGFR2 was localized at the membrane and in the cytoplasm, similar to FGFR2 localization in wild type XX gonads (Fig. 8, lower panel), demonstrating that SOX9, rather than SRY, is required for the nuclear localization of FGFR2. Thus SOX9 and FGFR2 seem linked, with the ability to re-inforce the action of one another. In a previous study, we demonstrated that *Sry* gene expression at E11.5 is unaffected in *Sox9* mutant XY gonads (Barrionuevo et al., 2006). Here we extend our findings to show that SRY protein expression and nuclear localization are also unaltered.

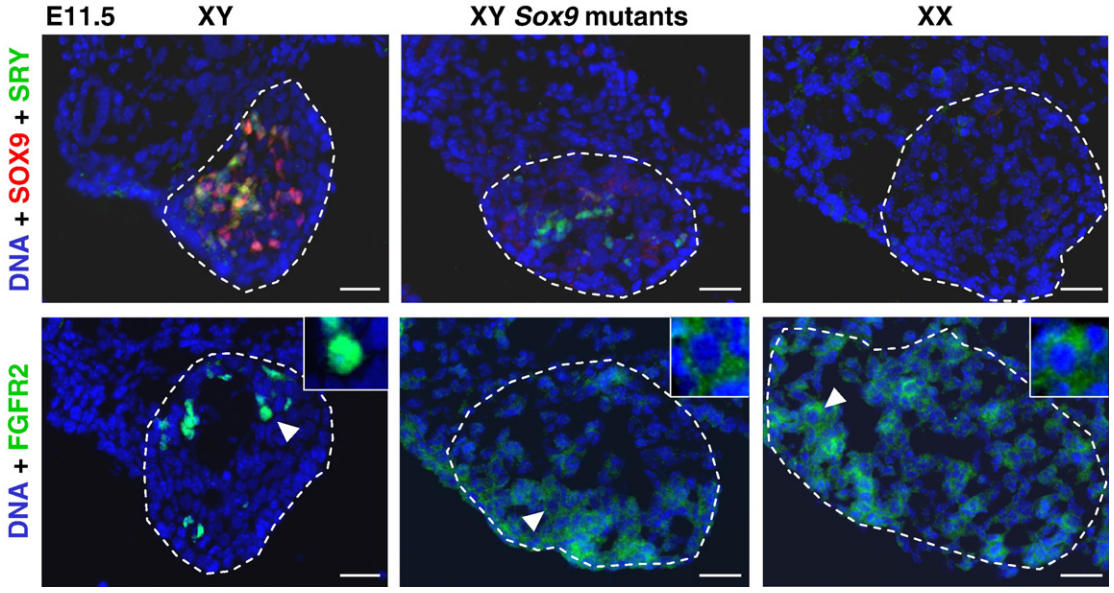

Fig. 8. SOX9 is required for nuclear localization of FGFR2. Fluorescence microscopy of frozen transverse sections of *Sox9* mutant XY and control embryos at early E11.5 (15 tail somites) double immunostained for SRY (green, nuclear) and SOX9 (red, nuclear) (upper panel), and immunostained for FGFR2 (lower panel). Dashed lines mark the perimeter of *Sox9* mutant XY and control gonads. The inserts in the lower panel show magnification of cells stained for DAPI (blue, nuclear) and FGFR2 (green, nuclear in the wild type XY gonad, cytoplasmic in the *Sox9* mutant XY gonad and in the wild type XX gonad). In *Sox9* mutant XY gonads, though SRY was expressed, FGFR2 was localized at the membrane and in the cytoplasm, similar to FGFR2 localization in wild type XX gonads. Note that FGFR2 nuclear localization is a dynamic process. At early E11.5, only a few FGFR2-positive nuclei are present within the gonad, while by late E11.5, that number has increased (Schmahl et al., 2004). Similarly, at early E11.5, FGFR2 expression at the XY coelomic epithelium is barely detectable, while by late E11.5, FGFR2 expression is much stronger (Schmahl et al., 2004). We could only examine early E11.5 XY wild type controls because most of the *Sox9* mutants do not survive beyond early E11.5. All scale bars are 50 μm.

Fgfr2/Sox9 double heterozygous knockout mice show partial XY gonadal sex reversal

Given that FGFR2 loss can lead to a drastic reduction in the number of SOX9-expressing cells (Fig. 5B(ii), bottom panel), and that FGFR2 nuclear localization is dependent on SOX9, we examined the functional relationship between FGFR2 and SOX9 *in vivo*. We generated double heterozygous *Fgfr2/Sox9* knockout mice (*CMV:Cre;Fgfr2*$^{floxdel/+}$*;Sox9*$^{flox/+}$) using the *CMV:Cre* mouse line (Schwenk et al., 1995).

Fgfr2/Sox9 knockout embryos were recovered at the expected Mendelian ratio, but died immediately after birth. In contrast to *Fgfr2* or *Sox9* single heterozygous mutant XY gonads which developed as normal testes (data not shown), double heterozygous *Fgfr2/Sox9* knockout XY gonads developed as ovotestes and were very similar in appearance to *Fgfr2* mutant XY gonads. Of 24 XY *Fgfr2/Sox9* knockout gonads between E12.5 and E15.5, 20 displayed ovotestes (6 at E12.5, 2 at E13.5, 10 at E14.5 and 2 at E15.5), while 4 (2 at E12.5 and 2 at E14.5) showed no defects in testis cord formation.

Immunohistochemistry of *Fgfr2/Sox9* knockout XY gonads at E12.5 showed that the number of SOX9- and AMH-positive cells was greatly reduced near the poles, particularly at the anterior pole (Fig. 9A(i), top and middle panels). By E14.5, SOX9 and AMH were completely absent at the poles, indicating a failure of Sertoli cell differentiation (Fig. 9A(ii)) similar to that of *Fgfr2* mutants (Fig. 3C). Remarkably, while strong nuclear FGFR2 expression was visible in the wild type XY male gonad, FGFR2 expression was barely detectable throughout the entire *Fgfr2/Sox9* knockout gonad (Fig. 9A(i), bottom panel). In contrast, *Fgfr2* or *Sox9* single heterozygous knockouts showed no obvious defects of SOX9 or FGFR2 immunostaining, respectively (data not shown). It appears that in *Fgfr2/Sox9* knockout gonads the SOX9–FGFR2 signaling loop is weakened to just below the threshold required to efficiently maintain nuclear FGFR2 expression, while SOX9 may still be maintained, most likely through the Prostaglandin signaling pathway.

The poles of *Fgfr2/Sox9* knockout XY gonads expressed the female somatic marker *Bmp2* (Fig. 9B, upper panel), and the meiosis markers SCP3 (Fig. 9B, lower panel) and *Dmc1* (data not shown), indicating that these regions of the gonad were sex reversed.

Discussion

XY gonadal dysgenesis in humans arises from mutations in testis-determining genes and duplications of anti-testis genes, which together explain some 20% of these DSD conditions, implying that a number of sex-determining genes remain undiscovered. FGF9 is essential for sex determination in mice and it is reasonable to postulate that FGF9 and its receptor(s) would be sex-determining genes in humans. We considered *Fgfr2* a candidate testis-determining gene, since (a) it encodes a potential receptor for FGF9 during male sex determination, (b) knockout mice of the other FGF receptors, FGFR1, FGFR3 and FGFR4 show no obvious gonadal phenotype and (c) FGFR2 protein shows male-specific localization in the nuclei of Sertoli cell precursors (Schmahl et al., 2004). Here, we successfully

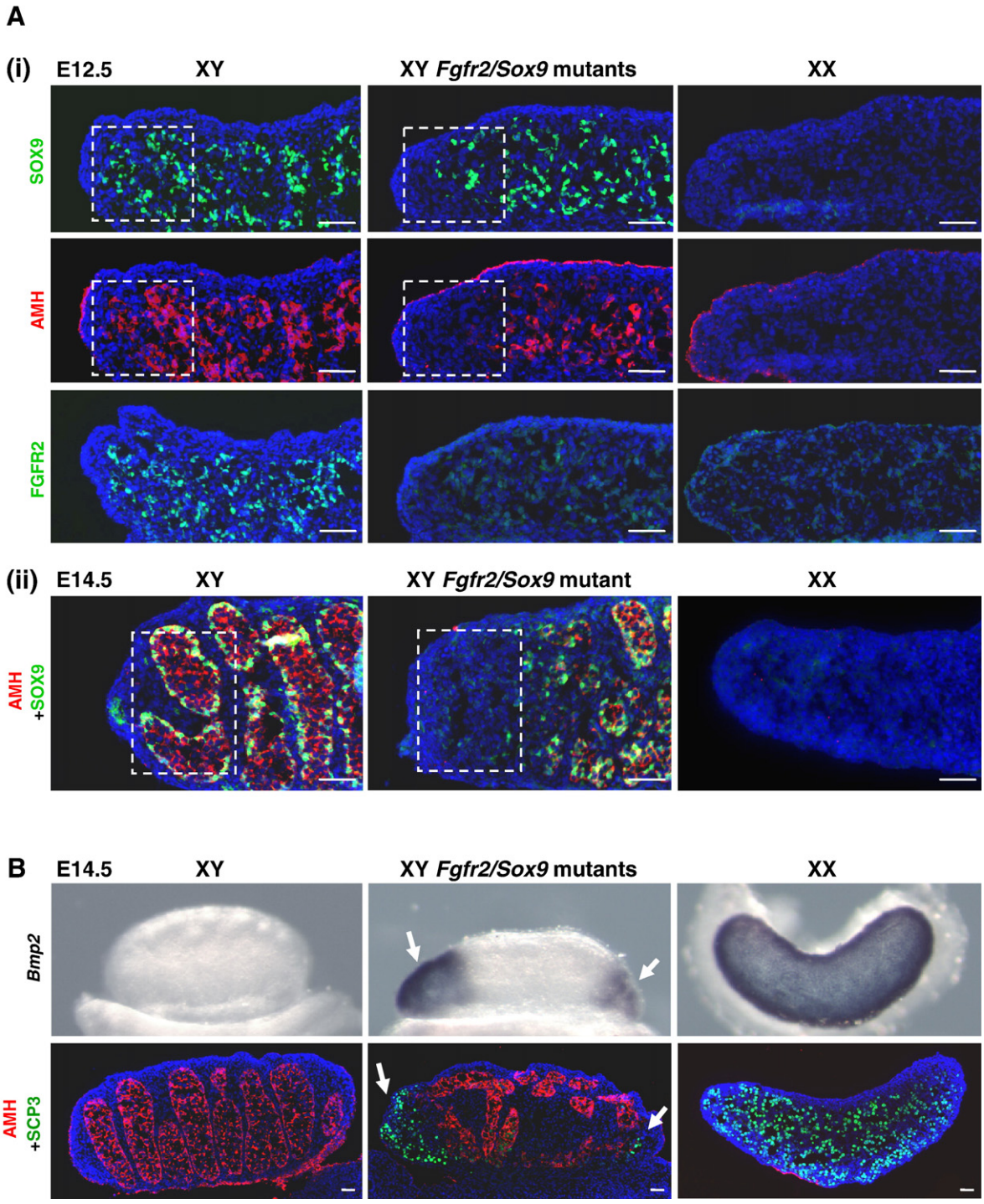

Fig. 9. *Fgfr2/Sox9* double heterozygous knockout mice show partial XY gonadal sex reversal. (A) (i) Fluorescence microscopy of frozen sections of *Fgfr2/Sox9* knockout and control gonads at E12.5 immunostained for SOX9 (green, nuclear) (top panel), AMH (red, cytoplasmic) (middle panel) and FGFR2 (green, nuclear) (bottom panel). Note that while SOX9 and AMH immunohistochemistry has been performed on the same gonad section, the sections immunostained for SOX9/AMH and FGFR2 are not consecutive. In *Fgfr2/Sox9* knockout gonads, the number of SOX9- and AMH-expressing cells was drastically reduced at the anterior pole (framed). Moreover, while XY control gonads show strong FGFR2 expression, FGFR2 is barely detectable throughout the entire *Fgfr2/Sox9* knockout gonad. (ii) Fluorescence microscopy of frozen sections of *Fgfr2/Sox9* knockout and control gonads at E14.5 double immunostained for SOX9 (green, nuclear) and AMH (red, cytoplasmic). By E14.5, SOX9 and AMH expression is absent from the poles of *Fgfr2/Sox9* knockout gonads (framed). (B) Upper panel: Whole mount *in situ* hybridization for *Bmp2* of E14.5 *Fgfr2/Sox9* knockout and control gonads. Arrows point to the *Bmp2*-positive poles of the *Fgfr2/Sox9* knockout gonad. Lower panel: Fluorescence microscopy of frozen sections of *Fgfr2/Sox9* knockout and control gonads at E14.5 double immunostained for AMH (red, cytoplasmic) and SCP3 (green, nuclear). Arrowheads denote SCP3-positive cells at the poles of the *Fgfr2/Sox9* knockout XY gonad. All scale bars are 50 μm.

used a *Ck19*-driven Cre-*loxP* system to inactivate *Fgfr2* specifically within the embryo proper (epiblast) (Means et al., 2005), circumventing the early embryonic lethality of complete *Fgfr2* knockout embryos.

Fgfr2 is required for male sex determination

In this study, we identify *Fgfr2* as an important player during male sex determination. *Fgfr2* mutant XY mice on a mixed 129/C57BL6-background had either normal testes, or showed partial sex reversal with ovarian tissue restricted to the gonad poles. However, one backcross to C57BL6 (B6), a mouse strain exquisitely sensitive to XY sex reversal, resulted in more dramatic XY sex reversal, with gonadal phenotypes ranging from hypoplastic testes and ovotestes, to gonads the size and shape of ovaries with an almost complete absence of Sertoli cells. Similarly, *Fgf9* knockout mice on a mixed 129/B6-background with unknown B6 contribution showed a wide range of gonadal phenotypes, from disorganized testis structures, to complete absence of testis-specific markers (Colvin et al., 2001). It may be speculated that further backcrosses to B6 would result in a more penetrant sex-reversal phenotype of *Fgfr2* mutant XY gonads as has been demonstrated for *Fgf9* knockout mice (Colvin et al., 2001; Schmahl et al., 2004). Given the remarkably similar phenotypes of *Fgfr2* mutant (129/B6*) and *Fgf9* knockout mice on a mixed 129/B6 background, and since typical male-specific FGF9-binding to the coelomic epithelium was abolished in *Fgfr2* mutant XY gonads, we suggest that FGFR2 acts as the receptor for FGF9 during male gonadal development. Recently, a SOX9–FGF9 positive signaling loop has been postulated in the male gonad (Kim et al., 2006). SOX9 initiates *Fgf9* transcription, and FGF9 maintains SOX9 expression and induces nuclear localization of FGFR2 in Sertoli cell precursors (Schmahl et al., 2004). Here, we extend these findings by showing directly that SOX9 is required for FGFR2 nuclear localization and conversely, that FGFR2 is important for the maintenance of SOX9 expression. These results suggest that FGFR2 and SOX9 regulate each other through a SOX9–FGF9–FGFR2 positive signaling loop. The molecular consequences of SOX9-mediated FGFR2 nuclear localization via FGF9 remain to be elucidated.

Just recently, a paper similar to ours has been published (Kim et al., 2007). The authors show that FGFR2 expression in both the coelomic epithelium and the Sertoli cells is important for testis development. In contrast to our data, early inactivation of *Fgfr2* always led to a complete XY sex-reversal phenotype. This difference of phenotype is most likely attributable to a different contribution of the B6 mouse strain.

The FGF9/FGFR2 and PGDS/PGD2 pathways appear to act independently to maintain SOX9 expression in the XY gonad

While XY *Fgfr2* mutant (129/B6*) ovotestes contain a majority of ovarian tissue, they still expressed SOX9 and AMH in the center. Similarly, in *Fgf9* knockout mice on a mixed 129/B6 background, over 50% of E13.5/E14.5 gonads displayed testis cords and robustly expressed SOX9 and AMH (Colvin et al., 2001). These two independent observations suggest that SOX9 expression is not solely dependent on FGFR2 or FGF9. Recently, a second positive signaling loop, PGDS–PGD2–SOX9, has been postulated to maintain SOX9 expression in the developing male gonad (Malki et al., 2005; Wilhelm et al., 2005, 2007). We found that *Pgds* was still strongly expressed in the SOX9-expressing center of *Fgfr2* mutant XY gonads, suggesting that the PGDS–PGD2 pathway can maintain SOX9 expression independently of FGFR2. However, the critical experiment to show that the Prostaglandin pathway can indeed maintain SOX9 expression in this system would be the analysis of double *Fgfr2/Pgds* knockout mice. At the poles of the gonad in the absence of FGFR2, the PGDS–PGD2 pathway apparently cannot efficiently maintain SOX9 expression. That SOX9, AMH, *Cyp26b1* and *Pgds* expression was lost specifically at the gonad poles may be attributable to the fact that SRY and SOX9 expression is strongest in the center of the gonad (Bullejos and Koopman, 2001; Schepers et al., 2003; Wilhelm et al., 2005), making the poles more sensitive to XY sex reversal. In accordance with our observations, ovotestes generally form with testicular tissue at the center and with ovarian tissue at the gonad poles (Eicher et al., 1980).

FGFR2 and human XY sex reversal

The demonstration of *Fgfr2* as a sex-determining gene in mice renders human *FGFR2* a candidate gene for unsolved DSD (disorders of sexual development) cases. Indeed, human patients with terminal deletions of chromosome 10q26 spanning the 10q26.13 region, which includes the *FGFR2* locus, show abnormal sexual differentiation, from micropenis and cryptorchidism, to partial XY sex reversal, and occasionally complete XY sex reversal with gonadal dysgenesis (Wilkie et al., 1993 and references therein). This suggests that the abnormal sexual phenotype in cases with terminal 10q26 deletions is associated with insufficient gene dosage (haploinsufficiency). The sex-reversal phenotype of double heterozygous *Fgfr2/Sox9* XY knockout mice also results from reduced levels of the FGFR2 protein, which supports the notion for a threshold activity of FGFR2 for normal testis development. Though mutations in human *FGFR2* have been well characterized and do not seem to result in XY sex reversal, these mutations alter the function of the FGF receptor 2 and do not lead to a loss of function as is the case for the *Fgfr2* knockout mice. Like *SOX9* gene mutations that cause XY sex reversal when heterozygous in humans but not in mice (Barrionuevo et al., 2006; Chaboissier et al., 2004; Foster et al., 1994; Wagner et al., 1994), we speculate that a heterozygous inactivating mutation in human *FGFR2* may lead to DSD, despite the fact that heterozygous *Fgfr2* mutant XY mice show a normal male phenotype. That *Sox9/Fgfr2* heterozygous mice show an intersex phenotype raises the possibility of compound heterozygous mutations/polymorphisms causing human DSD conditions.

Conclusion

We show that FGFR2 is important for male sex determination since (i) *Fgfr2* mutant XY mice show gonadal male-to-female sex

reversal and phenocopy *Fgf9* knockout mice when also on a mixed 129/C57BL6 background, (ii) *Fgfr2/Sox9* double heterozygous XY knockout mice show gonadal male-to-female sex reversal and (iii) FGF9 does not bind to the coelomic epithelium of *Fgfr2* mutant XY gonads. Taken together, our data support FGFR2 being the receptor for FGF9 during male sex determination.

Materials and methods

Mouse crosses

Generation of XY Ck19:Cre/+;Fgfr2$^{flox/flox}$ embryos

Fgfr2$^{flox/flox}$ (whose *Fgfr2* exons 8 and 10 are flanked by *loxP* sites) on a mixed 129/C57BL6 genetic background (Yu et al., 2003) were crossed with the *Ck19:Cre/+* (C57BL6) transgenic mouse line (Means et al., 2005). Resultant *Ck19:Cre/+;Fgfr2$^{flox/+}$* offspring were backcrossed to *Fgfr2$^{flox/flox}$* mice to obtain XY *Ck19:Cre/+;Fgfr2$^{flox/flox}$* embryos. The conditional *Fgfr2* allele interferes with the expression of both *Fgfr2-IIIb* and *Fgfr2-IIIc* isoforms (Yu et al., 2003).

Generation of XY Ck19:Cre/+;Fgfr2$^{flox/flox}$ embryos (129/B6)*

Ck19:Cre/+;Fgfr2$^{flox/+}$ and *Fgfr2$^{flox/flox}$* mice were crossed to C57BL6 for one generation. Resultant *Ck19:Cre/+;Fgfr2$^{flox/+}$*(129/B6*) and *Fgfr2$^{flox/+}$* (129/B6*) mice were crossed with each other to generate XY *Ck19:Cre/+;Fgfr2$^{flox/flox}$* embryos (129/B6*).

Generation of XY CMV:Cre;Fgfr2$^{floxdel/+}$;Sox9$^{flox/+}$ embryos

Male *CMV:Cre/+* mice (Schwenk et al., 1995) were crossed with female *Fgfr2$^{flox/flox}$* mice to obtain female *CMV:Cre;Fgfr2$^{floxdel/+}$* mice. These female mice were then crossed with *Sox9^{floxflox}* mice to generate XY *CMV:Cre;Fgfr2$^{floxdel/+}$;Sox9$^{flox/+}$* embryos.

Ck19:Cre/+;Sox9^{floxflox} embryos were generated as previously described (Barrionuevo et al., 2006).

Embryos were harvested at E11.5–E15.5 days gestation with day 0.5 designated as the morning the plug was identified. All procedures involving mice were approved by the Animal Ethics Committee of Monash University, Australia.

Genotyping of mouse embryos

Genomic DNA was isolated from the yolk sac for genotyping. Primers and PCR conditions for the *Cre* and *Sox9^{flox}* (Barrionuevo et al., 2006) and for *Fgfr2^{flox}* and *Fgfr2^{floxdel}* alleles (Yu et al., 2003) were used as previously described. Embryos were sexed by PCR using primers based on the mouse *Smcx* and *Smcy* genes as previously described (Barrionuevo et al., 2006).

Whole mount analyses of gonads

Embryos from E13.5 to E15.5 were collected in cold phosphate-buffered saline (PBS). The gonads were dissected out of the embryos, fixed in 4% PFA overnight at 4 °C and documented using a Zeiss Stemi SV11 stereomicroscope.

Histological analyses

For histology, embryos at E13.5 and E14.5 were collected in PBS, fixed in Serra (ethanol: 37% formaldehyde:acetic acid, 6:3:1) overnight at 4 °C, embedded in paraffin and sectioned at 5–6 μm. Staining of sections with hematoxylin and eosin followed standard techniques.

Cryosection and Immunofluorescence

Fetal gonads between E11.5 and E14.5 were dissected in PBS and fixed in 4% PFA/PBS for 3 h at 4 °C. They were washed twice in PBS, incubated for 1 h in 15% sucrose/PBS and then overnight in 30% sucrose/PBS at 4 °C. Samples were embedded in OCT medium (Tissue-Tek) and frozen at −70 °C, and serial 5 μm sections were cut with a cryostat (Leica) ((Gasca et al., 2002) with some modifications). Indirect immunofluorescence staining was performed using the primary antibodies to SOX9 (Morais da Silva et al., 1996), FGFR2 (Santa Cruz; sc-122), AMH (Santa Cruz; sc-6886), SCP3 (Abcam; ab15092) and SRY (Abcam; ab22166) with Alexa dye-linked secondary antibodies (Molecular Probes, Carlsbad, CA). Images were captured using fluorescence microscopy (Olympus Corp., NY).

In situ FGF9 binding assay

FGF9 *in situ* binding assays were performed as previously described (Schmahl et al., 2004). E11.5 frozen sections (12 μm) of XY control, XX control and XY *Fgfr2* mutant gonads were treated with human FGF9 protein (0.7 μg/ml) (R&D systems; AF-273-NA), which was detected by an antibody specific to human FGF9 (R&D systems; 273-F9).

Whole mount in situ hybridization

Gonads between E12.5 and E14.5 were dissected in DEPC treated PBS, fixed in 4% PFA/DEPC overnight at 4 °C, dehydrated through a methanol series and stored at −20 °C. Whole mount *in situ* hybridization of gonads with probes for *Wnt4* (Vainio et al., 1999), *Pgds* (kindly provided by Dagmar Wilhelm) and *Stra8*, *Dmc1*, *Cyp26b1*, *Fst* and *Bmp2* (kindly provided by Josephine Bowles) was performed as described (Zheng et al., 2001), with some modifications.

Acknowledgments

This work was supported by NHMRC (Australia) Grant 334314 to VRH. We thank David Ornitz for *Fgfr2$^{flox/flox}$* mice, Ursula Lichtenberg (Institute for Genetics, University of Cologne) for *CMV:Cre/+* mice, Moira O'Bryan and Kate Loveland for antibodies and Josephine Bowles and Dagmar Wilhelm for *in situ* probes.

References

Barrionuevo, F., Bagheri-Fam, S., Klattig, J., Kist, R., Taketo, M.M., Englert, C., Scherer, G., 2006. Homozygous inactivation of Sox9 causes complete XY sex reversal in mice. Biol. Reprod. 74, 195–201.

Bouma, G.J., Albrecht, K.H., Washburn, L.L., Recknagel, A.K., Churchill, G.A., Eicher, E.M., 2005. Gonadal sex reversal in mutant Dax1 XY mice: a failure to upregulate Sox9 in pre-Sertoli cells. Development 132, 3045–3054.

Bowles, J., Knight, D., Smith, C., Wilhelm, D., Richman, J., Mamiya, S., Yashiro, K., Chawengsaksophak, K., Wilson, M.J., Rossant, J., et al., 2006. Retinoid signaling determines germ cell fate in mice. Science 312, 596–600.

Brennan, J., Capel, B., 2004. One tissue, two fates: molecular genetic events that underlie testis versus ovary development. Nat. Rev., Genet. 5, 509–521.

Bullejos, M., Koopman, P., 2001. Spatially dynamic expression of Sry in mouse genital ridges. Dev. Dyn. 221, 201–205.

Bullejos, M., Koopman, P., 2004. Germ cells enter meiosis in a rostro-caudal wave during development of the mouse ovary. Mol. Reprod. Dev. 68, 422–428.

Chaboissier, M.C., Kobayashi, A., Vidal, V.I., Lutzkendorf, S., van de Kant, H.J., Wegner, M., de Rooij, D.G., Behringer, R.R., Schedl, A., 2004. Functional analysis of Sox8 and Sox9 during sex determination in the mouse. Development 131, 1891–1901.

Chuma, S., Nakatsuji, N., 2001. Autonomous transition into meiosis of mouse fetal germ cells in vitro and its inhibition by gp130-mediated signaling. Dev. Biol. 229, 468–479.

Colvin, J.S., Bohne, B.A., Harding, G.W., McEwen, D.G., Ornitz, D.M., 1996. Skeletal overgrowth and deafness in mice lacking fibroblast growth factor receptor 3. Nat. Genet. 12, 390–397.

Colvin, J.S., Green, R.P., Schmahl, J., Capel, B., Ornitz, D.M., 2001. Male-to-female sex reversal in mice lacking fibroblast growth factor 9. Cell 104, 875–889.

Deng, C., Wynshaw-Boris, A., Zhou, F., Kuo, A., Leder, P., 1996. Fibroblast growth factor receptor 3 is a negative regulator of bone growth. Cell 84, 911–921.

Deng, C., Bedford, M., Li, C., Xu, X., Yang, X., Dunmore, J., Leder, P., 1997. Fibroblast growth factor receptor-1 (FGFR-1) is essential for normal neural tube and limb development. Dev. Biol. 185, 42–54.

Di Carlo, A.D., Travia, G., De Felici, M., 2000. The meiotic specific synaptonemal complex protein SCP3 is expressed by female and male primordial germ cells of the mouse embryo. Int. J. Dev. Biol. 44, 241–244.

Eicher, E.M., Beamer, W.G., Washburn, L.L., Whitten, W.K., 1980. A cytogenetic investigation of inherited true hermaphroditism in BALB/cWt mice. Cytogenet. Cell Genet. 28, 104–115.

Fleming, A., Vilain, E., 2005. The endless quest for sex determination genes. Clin. Genet. 67, 15–25.

Foster, J.W., Dominguez-Steglich, M.A., Guioli, S., Kowk, G., Weller, P.A., Stevanovic, M., Weissenbach, J., Mansour, S., Young, I.D., Goodfellow, P.N., et al., 1994. Campomelic dysplasia and autosomal sex reversal caused by mutations in an SRY-related gene. Nature 372, 525–530.

Gasca, S., Canizares, J., De Santa Barbara, P., Mejean, C., Poulat, F., Berta, P., Boizet-Bonhoure, B., 2002. A nuclear export signal within the high mobility group domain regulates the nucleocytoplasmic translocation of SOX9 during sexual determination. Proc. Natl. Acad. Sci. U. S. A. 99, 11199–11204.

Harley, V.R., Jackson, D.I., Hextall, P.J., Hawkins, J.R., Berkovitz, G.D., Sockanathan, S., Lovell-Badge, R., Goodfellow, P.N., 1992. DNA binding activity of recombinant SRY from normal males and XY females. Science 255, 453–456.

Hilscher, B., Hilscher, W., Bulthoff-Ohnolz, B., Kramer, U., Birke, A., Pelzer, H., Gauss, G., 1974. Kinetics of gametogenesis: I. Comparative histological and autoradiographic studies of oocytes and transitional prospermatogonia during oogenesis and prespermatogenesis. Cell Tissue Res. 154, 443–470.

Hughes, I.A., Houk, C., Ahmed, S.F., Lee, P.A., LWPES Consensus Group, ESPE Consensus Group, 2006. Consensus statement on management of intersex disorders. Arch. Dis. Child. 91, 554–563.

Kim, Y., Capel, B., 2006. Balancing the bipotential gonad between alternative organ fates: a new perspective on an old problem. Dev. Dyn. 235, 2292–2300.

Kim, Y., Kobayashi, A., Sekido, R., DiNapoli, L., Brennan, J., Chaboissier, M.C., Poulat, F., Behringer, R.R., Lovell-Badge, R., Capel, B., 2006. Fgf9 and Wnt4 act as antagonistic signals to regulate mammalian sex determination. PLoS Biol. 4, e187.

Kim, Y., Bingham, N., Sekido, R., Parker, K.L., Lovell-Badge, R., Capel, B., 2007. Fibroblast growth factor receptor 2 regulates proliferation and Sertoli differentiation during male sex determination. Proc. Natl. Acad. Sci. U. S. A. 104, 16558–16563.

Koubova, J., Menke, D.B., Zhou, Q., Capel, B., Griswold, M.D., Page, D.C., 2006. Retinoic acid regulates sex-specific timing of meiotic initiation in mice. Proc. Natl. Acad. Sci. U. S. A. 103, 2474–2479.

Malki, S., Nef, S., Notarnicola, C., Thevenet, L., Gasca, S., Mejean, C., Berta, P., Poulat, F., Boizet-Bonhoure, B., 2005. Prostaglandin D2 induces nuclear import of the sex-determining factor SOX9 via its cAMP-PKA phosphorylation. EMBO J. 24, 1798–1809.

McLaren, A., Southee, D., 1997. Entry of mouse embryonic germ cells into meiosis. Dev. Biol. 187, 107–113.

Means, A.L., Chytil, A., Moses, H.L., Coffey, R.J., Wright, C.V., Taketo, M.M., Grady, W.M., 2005. Keratin 19 gene drives Cre recombinase expression throughout the early postimplantation mouse embryo. Genesis 42, 23–27.

Meeks, J.J., Crawford, S.E., Russell, T.A., Morohashi, K., Weiss, J., Jameson, J.L., 2003. Dax1 regulates testis cord organization during gonadal differentiation. Development 130, 1029–1036.

Menke, D.B., Koubova, J., Page, D.C., 2003. Sexual differentiation of germ cells in XX mouse gonads occurs in an anterior-to-posterior wave. Dev. Biol. 262, 303–312.

Morais da Silva, S., Hacker, A., Harley, V., Goodfellow, P., Swain, A., Lovell-Badge, R., 1996. Sox9 expression during gonadal development implies a conserved role for the gene in testis differentiation in mammals and birds. Nat. Genet. 14, 62–68.

Ornitz, D.M., Xu, J., Colvin, J.S., McEwen, D.G., MacArthur, C.A., Coulier, F., Gao, G., Goldfarb, M., 1996. Receptor specificity of the fibroblast growth factor family. J. Biol. Chem. 271, 15292–15297.

Schepers, G., Wilson, M., Wilhelm, D., Koopman, P., 2003. SOX8 is expressed during testis differentiation in mice and synergizes with SF1 to activate the Amh promoter in vitro. J. Biol. Chem. 278, 28101–28108.

Schmahl, J., Kim, Y., Colvin, J.S., Ornitz, D.M., Capel, B., 2004. Fgf9 induces proliferation and nuclear localization of FGFR2 in Sertoli precursors during male sex determination. Development 131, 3627–3636.

Schwenk, F., Baron, U., Rajewsky, K., 1995. A cre-transgenic mouse strain for the ubiquitous deletion of loxP-flanked gene segments including deletion in germ cells. Nucleic Acids Res. 23, 5080–5081.

Sinclair, A.H., Berta, P., Palmer, M.S., Hawkins, J.R., Griffiths, B.L., Smith, M.J., Foster, J.W., Frischauf, A.M., Lovell-Badge, R., Goodfellow, P.N., 1990. A gene from the human sex-determining region encodes a protein with homology to a conserved DNA-binding motif. Nature 346, 240–244.

Swain, A., Lovell-Badge, R., 1999. Mammalian sex determination: a molecular drama. Genes Dev. 13, 755–767.

Vainio, S., Heikkila, M., Kispert, A., Chin, N., McMahon, A.P., 1999. Female development in mammals is regulated by Wnt-4 signalling. Nature 397, 405–409.

Wagner, T., Wirth, J., Meyer, J., Zabel, B., Held, M., Zimmer, J., Pasantes, J., Bricarelli, F.D., Keutel, J., Hustert, E., et al., 1994. Autosomal sex reversal and campomelic dysplasia are caused by mutations in and around the SRY-related gene SOX9. Cell 79, 1111–1120.

Weinstein, M., Xu, X., Ohyama, K., Deng, C.X., 1998. FGFR-3 and FGFR-4 function cooperatively to direct alveogenesis in the murine lung. Development 125, 3615–3623.

Wilhelm, D., Martinson, F., Bradford, S., Wilson, M.J., Combes, A.N., Beverdam, A., Bowles, J., Mizusaki, H., Koopman, P., 2005. Sertoli cell differentiation is induced both cell-autonomously and through prostaglandin signaling during mammalian sex determination. Dev. Biol. 287, 111–124.

Wilhelm, D., Hiramatsu, R., Mizusaki, H., Widjaja, L., Combes, A.N., Kanai, Y., Koopman, P., 2007. SOX9 regulates prostaglandin D synthase gene transcription in vivo to ensure testis development. J. Biol. Chem. 282, 10553–10560.

Wilkie, A.O., Campbell, F.M., Daubeney, P., Grant, D.B., Daniels, R.J., Mullarkey, M., Affara, N.A., Fitchett, M., Huson, S.M., 1993. Complete and partial XY sex reversal associated with terminal deletion of 10q: report of 2 cases and literature review. Am. J. Med. Genet. 46, 597–600.

Xu, X., Weinstein, M., Li, C., Naski, M., Cohen, R.I., Ornitz, D.M., Leder, P., Deng, C., 1998. Fibroblast growth factor receptor 2 (FGFR2)-mediated reciprocal regulation loop between FGF8 and FGF10 is essential for limb induction. Development 125, 753–765.

Yao, H.H., Matzuk, M.M., Jorgez, C.J., Menke, D.B., Page, D.C., Swain, A., Capel, B., 2004. Follistatin operates downstream of Wnt4 in mammalian ovary organogenesis. Dev. Dyn. 230, 210–215.

Yu, K., Xu, J., Liu, Z., Sosic, D., Shao, J., Olson, E.N., Towler, D.A., Ornitz, D.M., 2003. Conditional inactivation of FGF receptor 2 reveals an essential role for FGF signaling in the regulation of osteoblast function and bone growth. Development 130, 3063–3074.

Zheng, W., Izaki, J., Furusawa, S., Yoshimura, Y., 2001. A sensitive non-radioactive in situ hybridization method for the detection of chicken IgG gamma-chain mRNA: a technique suitable for detecting of variety of mRNAs in tissue sections. Biol. Proced. Online 3, 1–7.